In-Vivo Organ Perfusion Characterization with Dynamic Contrast-Enhanced Micro-CT

Marco Caballo[1], Sofia Koustoulidou[1], Addison Hunt[1], Pierluca Pitacco[1], Ruud M. Ramakers[1-2]

[1] **MILabs B.V., Houten, the Netherlands**
[2] **Radiation Detection and Medical Imaging, Delft University of Technology, Delft, The Netherlands**
Correspondence: applicationsupport@milabs.com

Introduction

In-vivo dynamic contrast-enhanced micro-CT (DCE-μCT) is an X-ray-based imaging modality aimed at the non-invasive spatiotemporal characterization of organs, tissues, and lesions. In typical DCE-μCT protocols, multiple three-dimensional (3D) frames are acquired over a given time range after the anesthetized animal undergoes intravenous injection of radiosensitive contrast-enhancing material. Each of these time frames captures a different moment of uptake, accumulation, or clearance of the contrast-enhancing material, resulting in a four-dimensional (4D) image showing the anatomy and perfusion of organs, tissues, and (if present) lesions.

Years of technological advancements in X-ray tube design, detector performance characteristics, and system geometry have allowed DCE-μCT to achieve resolution capabilities (both spatially and temporally) that are hardly matched by other imaging modalities. Furthermore, the attenuation of X-rays in organs and tissues is related in a linear fashion to the accumulation of contrast medium. This results in accurate, and absolute, image quantification that can ease the translation of preclinical research into clinics. [1]-[2]

Thanks to its quantification capabilities, coupled with a micrometer-level spatial resolution and a scan time of the order of a few seconds per frame, DCE-μCT finds applications in several preclinical research fields. Examples include tumor and *in-vivo* organ perfusion, hypoxia, and heterogeneity assessment [2]-[4], cancer therapy response evaluation and disease progression [5]-[6], efficacy of metallic theranostics nanoparticles [7]-[8], novel contrast agent development [9]-[11], and validation of image analysis and quantification methodologies and algorithms [12]-[13]. Furthermore, and in addition to its standalone use, DCE-μCT can also be paired with other imaging modalities and serve as an adjuvant technology to extract complementary information on organ physiology and disease processes (for example, by the simultaneous capture of perfusion and metabolic information when used in combination with nuclear imaging). [1]

In this white paper, we present an *in-vivo* example of DCE-μCT application for total body mouse perfusion imaging using the MILabs μCT (U-CT), and we describe experimental setup, image acquisition, reconstruction, and analysis settings.

Materials and Methods

All animal experiments were approved by the Animal Welfare Committee of the UMC Utrecht (the Netherlands), and all procedures were conducted according to the local rules and regulations. *In vivo* imaging of a wild-type C57BL/6 healthy mouse (body weight 20.2 grams) was performed using a preclinical μCT system (XUHR-μCT, MILabs, Houten, the Netherlands). A fast, single-energy total body protocol with continuous 360-degree gantry rotation and 2x2 binning was selected, with tube voltage, current, and exposure time being 50 kV, 0.21 mA, and 20 ms, respectively. Image acquisition was performed dynamically over 200 frames (9 sec/frame, 30 min total scan time).

Low-energy filtration was performed with the standard filters featured by the µCT system (Al 0.4 mm + Al 0.1 mm).

Before image acquisition, the animal was anesthetized (4% isoflurane) and subsequently placed in a prone position on a dedicated mouse bed (MILabs). The animal was kept under anesthesia for the duration of the scan (1% isoflurane, 200 mL/min).

A volume of 10 µL per gram of body weight of a commercially available contrast agent (ExiTron Nano 12000 NanoPET, Berlin, Germany) was prepared and injected with a 30G needle through the lateral tail vein (200 µL total injected volume). The contrast agent was injected through a custom-made catheter line after the acquisition of the first CT frame, and the remaining was flushed with saline after 9 minutes.

After image acquisition, all frames were reconstructed with a standard Feldkamp algorithm with Hann filtering at an isotropic voxel size of 120 µm, and denoised with a 360 µm (full-width-half-maximum, FWHM) isotropic Gaussian filter.

Immediately after the dynamic scan acquisition, and without moving the animal, an additional static total body scan was performed in ultra-focused magnification, accurate mode, and full scan angle with an angular step of 0.25 degrees. Tube voltage, current and exposure time were 50 kV, 0.21 mA, and 70 ms, respectively. This scan was reconstructed with the same algorithm as the previous scan at an isotropic voxel size of 30 µm, and denoised with a 120 µm (FWHM) isotropic Gaussian filter.

From the ultra-focused scan, segmentation of the heart, kidneys, spleen, bladder, and liver was obtained semi-automatically, through a combination of thresholding, morphological operators, and manual adjustment. These segmentation masks were subsequently translated into the respective anatomical locations on the dynamic scan. The aorta and

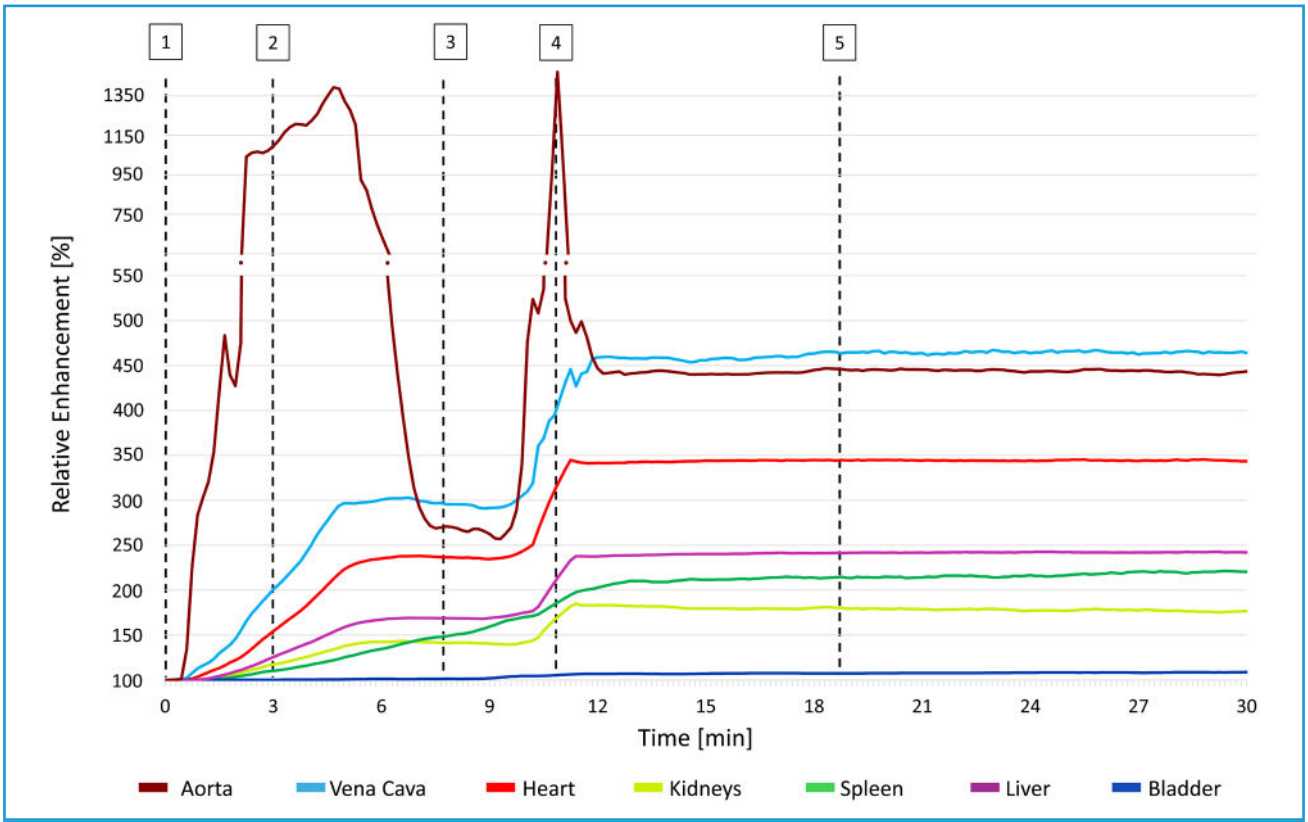

Figure 1. Perfusion curves (expressed in relative enhancement) for the organs and blood vessels evaluated in this study. The contrast agent injection was performed at 9 s after the start of the scan and after completing the first frame. The I.V. catheter was flushed at 9 min. The vertical axis is presented with two different scales in the upper and lower part, to improve visualization.

the inferior vena cava were instead segmented from the 34th frame of the dynamic scan (i.e., 5 minutes after injection), corresponding to the highest aortic enhancement, to maximize the contrast between arteries and veins.

From all segmentation maps, the average perfusion curve was calculated over the 200 frames, and denoised temporally with a moving average filter (window width of 7 frames). Quantitative perfusion parameters (time to peak (TTP), peak enhancement (PE), and wash-in rate (WI)) were then calculated from each curve, both after injection and after flushing the line.

All image analysis experiments were performed with Imalytics Preclinical 3.0 (Gremse-IT, Aachen, Germany), and MATLAB (The MathWorks, Natick, MA, USA).

Results and Conclusion

The extracted perfusion curves and the quantitative perfusion parameters are reported in Figure 1 and Table 1, respectively. Five representative image frames are shown in Figure 2.

The aorta showed the highest and fastest uptake (almost 9 times faster than the heart), with a trend typical of arterial input functions. Besides the aorta, the vena cava and heart showed the highest and fastest enhancement, followed by the liver, spleen, and kidneys. This is apparent by looking at the quantitative wash-in rate values (Table 1) for the first section of the curves, confirming that the μCT used in this study was able to characterize and quantify the inflow of contrast agent in the mouse body: first in the vein (site of injection), followed by the heart, and then to the other organs, as expected.

The bladder showed negligible contrast agent uptake. This is expected and is in line with the characteristics of the contrast agent used, since its relatively large nanoparticle size (~110 nm) hinders its excretion by the kidneys into bladder and promotes accumulation in the liver (in Kupffer cells) and spleen (in macrophages). This characteristic also allows the contrast agent to circulate for a long time, as apparent by the

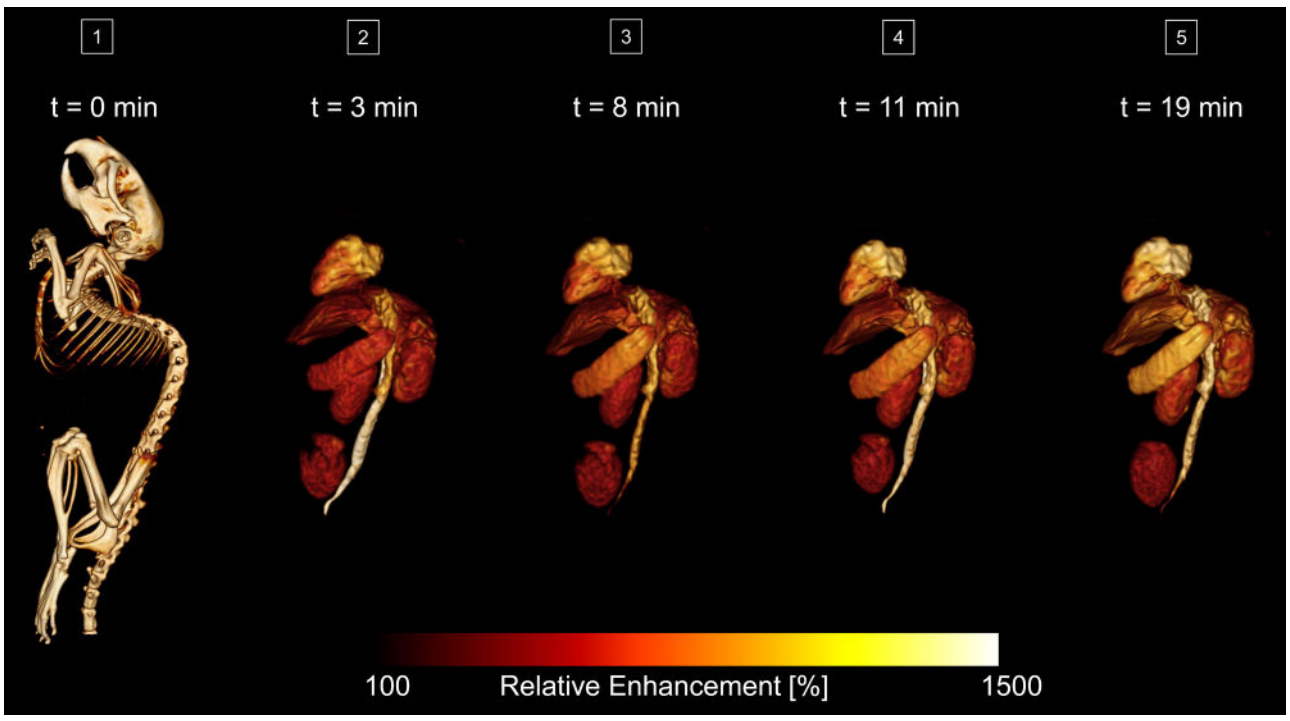

Figure 2. Five representative 3D image frames corresponding to the five moments numbered on the perfusion curves shown in Figure 1. To ease visualization, the mouse skeleton was removed in all post-contrast injection frames, and only the organs of interest are shown. The color scale was kept consistent for all frames.

organs maintaining a stable plateau as depicted in Figure 1 from 12 minutes onwards until the end of the scan. [14]-[15]

All organs showed a first uptake phase after contrast agent administration and a second rapid enhancement after flushing. An exception is constituted by the spleen, whose contrast uptake gradually increases monotonically at approximately the same rate for the whole duration of the scan. This is likely due to the slow uptake of spleen macrophages, where the contrast medium tends to accumulate [16].

In conclusion, the μCT used in this study, thanks to its exquisite spatiotemporal resolution capabilities, successfully characterized and quantified the perfusion of different organs and blood vessels in a mouse model. This can find application in all biomedical research fields requiring a dynamic analysis of organs and structures, including (but not limited to) oncology, cardiology, pharmacokinetics, drug delivery, treatment response assessment, and new contrast agent development and validation.

Table 1. Quantitative perfusion parameters calculated from each perfusion curve, in the first (after injection, before flush) and second section (after flush). The wash-in rate was calculated as the ratio between the peak enhancement and the time-to-peak (adjusted for the relative start of each section, 9 s and 9 min). PE = peak enhancement; TTP = time-to-peak; WI = wash-in rate.

		Aorta	Vena Cava	Heart	Kidneys	Spleen	Liver	Bladder
First Section	PE [a.u.]	13.93	3.09	2.38	1.43	1.59	1.69	1.02
	TTP [min]	4.65	6.75	7.05	6.6	9	6.75	9
	WI * [min^{-1}]	3.0	0.45	0.34	0.22	0.18	0.25	0.11
Second Section	PE [a.u.]	14.71	4.59	3.45	1.85	2.21	2.38	1.06
	TTP [min]	10.8	12	11.25	11.4	29.4	11.55	11.85
	WI ** [min^{-1}]	8.17	1.53	1.53	0.77	0.11	0.93	0.37

$*\ WI = {}^{PE}/_{TTP} \qquad **\ WI = {}^{PE}/_{(TTP-9)}$

References

[1] S. Koyasu, et al. Evaluation of Tumor-associated Stroma and Its Relationship with Tumor Hypoxia Using Dynamic Contrast-enhanced CT and (18) F Misonidazole PET in Murine Tumor Models. Radiology 2016;278(3):734-41

[2] M. Braunagel, et al. Dynamic Contrast-Enhanced Computed Tomography: A New Diagnostic Tool to Assess Renal Perfusion After Ischemia-Reperfusion Injury in Mice: Correlation of Perfusion Deficit to Histopathologic Damage. Invest Radiol 2016;51(5):316-22

[3] R. Margolis, et al. Comparison of micro-CT image enhancement after use of different vascular casting agents. Quant Imaging Med Surg 2024;14(3):2568-2579

[4] V. Kersemans, et al. Improving In Vivo High-Resolution CT Imaging of the Tumour Vasculature in Xenograft Mouse Models through Reduction of Motion and Bone-Streak Artefacts. PLoS One 2015;10(6):e0128537

[5] J. Xu, et al. Fabrication of multifunctional polydopamine-coated gold nanobones for PA/CT imaging and enhanced synergistic chemo-photothermal therapy. Journal of Materials Science & Technology 2021;63:97-105

[6] T. Pöschinger, et al. Dynamic contrast-enhanced micro-computed tomography correlates with 3-dimensional fluorescence ultramicroscopy in antiangiogenic therapy of breast cancer xenografts. Invest Radiol 2014;49(7):445-56

[7] Q. Bao, et al. Enhanced Cancer Imaging and Chemo-Photothermal Combination Therapy by Cancer-Targeting Bismuth-Based Nanoparticles. Adv. Optical Mater. 2023;11(11):2201482

[8] R. Rizzo, et al. Bi-HPDO3A as a novel contrast agent for X-ray computed tomography. Scientific

Reports 2023;13:16747

[9] Y. C. Dong, et al. Effect of Gold Nanoparticle Size on Their Properties as Contrast Agents for Computed Tomography. Scientific Reports 2019;9:14912

[10] K. Ramesh et al. Ligand-Specific Nano-Contrast Agents Promote Enhanced Breast Cancer CT Detection at 0.5 mg Au. Int J Mol Sci 2022;23(17):9926

[11] J. Kim, et al. Radioprotective garment-inspired biodegradable polymetal nanoparticles for enhanced CT contrast production. Chem Mater 2020;32(1):381-391

[12] G. Z Ferl, et al. Automated segmentation of lungs and lung tumors in mouse micro-CT scans. iScience 2022;25(12):105712

[13] D. Yan, et al. A Novel Mouse Segmentation Method Based on Dynamic Contrast Enhanced Micro-CT Images. PLoS One 2017;12(1):e0169424

[14] https://www.viscover-online.de/ct-porfolio/exitron-nano-12000/a-163/

[15] J. Toczek, et al. Computed tomography imaging of macrophage phagocytic activity in abdominal aortic aneurysm. Theranostics 2021;11(12):5876-5888

[16] J. G. Mannheim, et al. Comparison of small animal CT contrast agents. Contrast Media Mol Imaging 2016;11(4):272-84